Supporting Information for:

Chromate reduction in Fe(II)-containing soil affected by hyperalkaline leachate from chromite ore processing residue

Robert A. Whittleston[1], Douglas I. Stewart[2*], Robert J. G. Mortimer[1], Zana C. Tilt[1], Andrew P. Brown[3], Kalotina Geraki[4], and Ian T. Burke[1*].

[1] School of Earth and Environment, [2] School of Civil Engineering, [3] School of Process, Environmental and Materials Engineering, University of Leeds, Leeds LS2 9JT, UK

[4] Diamond Light Source, Harwell Science and Innovation Campus, Didcot, Oxfordshire, OX11 0DE, UK

[*] Corresponding Author's E-mail: i.burke@see.leeds.ac.uk / d.i.stewart@leeds.ac.uk

This section consists of 13 pages, 4 tables, and 3 figures.

Section 1. Sample characterisation.

X-ray powder diffraction (XRD) analysis of the soils (ground to < 75 μm) was performed on a Philips PW1050 Goniometer, and X-ray fluorescence (XRF) analysis was undertaken using a fused sample on a Philips PW2404 wavelength dispersive sequential X-ray spectrometer (data were corrected for loss on ignition). Approximately 25g of homogenised soil was oven dried at 105°C and disaggregated with a mortar and pestle for carbon content determination. A portion of each sample was pre-treated with 10% HCl to remove any carbonates present [1]. The total organic and inorganic carbon contents of oven dried and HCl treated subsamples were measured using Carlo-Erba 1106 elemental analyser.

Soil pH was measured following the ASTM standard method for pH in soils, with 10g soil made up to a 1:1 suspension with deionised water. The suspension was left for 1 hour before measurement was taken using a Orion bench top meter and calibrated electrodes [2]. Water soluble Cr(VI) content in soils was measured using 10:1 suspension of soil to deionised water, shaken for 24 hours at 150

rpm in 15ml centrifuge tubes. 1.5 ml was then extracted and centrifuged (3 min, 16,000 g). Aqueous Cr(VI) concentration in the supernatant was then determined using standard UV/VIS spectroscopy methods based described in main paper [3].

A freeze dried sample of soil from B2 310 was embedded in a block of epoxy resin under a vacuum and prepared for SEM analysis by polishing in non-aqueous oils and carbon coating (approximately 5-10 nm thickness). Scanning Electron Microscopy (SEM) was performed on a FEI Quanta 650 FEG-ESEM to produce backscatter electron images. Elemental quantification was carried out on the ESEM using an electron probe micro analyser (EPMA). Thirty-three 15 x 15 µm regions of the fine matrix material of B2 310 resin embedded thin section were analysed for common rock forming oxides. The measured elemental wt% were then corrected by assuming a total oxide weight of 100% to account for the influence of resin infilling into pore spaces. An average composition of these 33 regions is reported in the results section, with error given as the range of the results.

Soil B2 310 was prepared for (S)TEM imaging by freeze drying and sieving at 150 mesh to collect the less than 104 µm sized fraction. Approximately 0.05 g was then mixed with 1 ml of LR White^{TM} resin and polymerised for 24 hours at 70°C. A thin section of resin embedded soil was then cut using a microtome (80 nm) and placed on a Cu support grid (Agar Scientific, UK) and carbon coated (~5 um) prior to (S)TEM analysis. The specimen was examined using a Philips/FEI CM200 field emission gun TEM fitted with a scanning (STEM) unit and an ultra thin window energy dispersive X-ray detector (Oxford Instruments ISIS EDX). The total Cr concentration in this soil was ~0.3 % w/w, which if homogeneously dispersed is close to the limit of detection for EDX analysis.

Section 2. XAS analysis.

Samples for XAS analysis were chosen from a range of borehole samples, and from reoxidation experiments on soil B2-310. , Soil slurry from one reoxidation experiment was centrifuged (10 min, 8,000 g), and the soil was recovered and stored in the dark at -80°C. All other samples for XAS analysis were stored at -80°C in the dark under a nitrogen atmosphere.

Cr K-edge spectra were collected on beamline I18 at the Diamond Light Source in November 2009, operating at 3 GeV with a typical current of 200 mA, using a nitrogen cooled Si(111) double crystal monochromator and focussing optics. A pair of plane mirrors was used to reduce the harmonic content of the beam and microfocusing was done using Kirkpatrick-Baez mirrors. The

beam size at the sample was approximately 150 µm. For standards the Cr K-edge spectra were collected in transmission mode at room temperatures (~295 °K). Standards were prepared as 50 mg pressed pellets and diluted with BN as required. For soil samples data were collected in fluorescence mode using a 9 element solid state Ge detector. Soil samples were centrifuged to form a moist pellet and were mounted at 1 mm thickness in aluminium holders with Kapton™ widows. Experiments were performed at liquid nitrogen temperatures (approximately 78 °K) and multiple scans averaged to improve the signal to noise ratio using Athena version 0.8.056 [4]. For XANES spectra absorption was also normalised in Athena over the full data range and plotted from 5980 eV to 6030 eV with no correction required for drift in E_0. For EXAFS analysis data was background subtracted using PySpline v1.1 [5].

Section 3 EXAFS Analysis.

Background subtracted EXAFS spectra were analysed in DLexcurv v1.0 [6] using full curved wave theory [7]. Phaseshifts were derived from *ab initio* calculations using Hedin-Lundqvist potentials and von-Barth ground states [8]. Fourier transforms of the EXAFS spectra were used to obtain an approximate radial distribution function around the central Cr atom (the absorber atom); the peaks of the Fourier transform can be related to "shells" of surrounding backscattering ions characterised by atom type, number of atoms, absorber-scatterer distance, and the Debye-Waller factor (± 25%), $2\sigma^2$. Atomic distances calculated by DLexcurv have an error of approximately ± 0.02 and ± 0.05 Å in the first and outer shells respectively [9]. The data were fitted for each sample by defining a theoretical model and comparing the calculated EXAFS spectrum with experimental data and with published spectra for Cr-substituted compounds [10]. Shells of backscatterers were added around the Cr and by refining an energy correction Ef (the Fermi Energy; which for final fits typically varied between -19 and -17), the absorber-scatterer distance, and the Debye-Waller factor for each shell, a least squares residual (the *R* factor [11]) was minimised. The amplitude factor (or AFAC in DLexcurv V1.0) was retained as the default of 1 throughout. Shells or groups of shells were only included if the overall fit (*R*-factor) was reduced overall by >5%. For shells of scatterers around the central Cr, the number of atoms in the shell was chosen as an integer to give the best fit and further refined.

Section 4 Microbial community analysis.

4.1 Iron reducing alkaline media

To culture alkaliphilic anaerobic iron reducers indigenous to the B2 310 soil layer an alkaline media containing Fe(III) was developed. The base media contained $NaH_2PO_4.H_2O$ (0.356 g/l), KCl (0.1 g/l) and 10 ml of standard vitamin and mineral mixtures [12]. Fe(III) citrate (2 g/l) and yeast extract (2 g/l) were added as the sole sources of electron acceptors and donors. The media was made using DIW that was first deoxygenated by boiling and nitrogen purging. The pH was adjusted to 9.2 using a 1M solution of sodium carbonate and 4.5 ml aliquots transferred to 5 ml glass serum bottles. These were then sealed using butyl rubber stoppers and aluminium crimps, and heat sterilised at 120°C for 20 minutes.

4.2. DNA extraction and cloning procedure

Microbial DNA was extracted from a 400 mg sample of B2-310 initial soil using a FastDNA spin kit (Qbiogene, Inc.) and FastPREP instrument (unless explicitly stated, the manufacturer's protocols supplied with all kits employed were followed precisely). In order to extract microbial DNA from the iron reducing consortiums, a culture bottle was opened, transferred into a 15 ml centrifuge tube and centrifuged at 3500 rpm for 10 minutes. Supernatant was then discarded and pellet resuspended in 978 µl of sodium phosphate buffer supplied in the FastDNA spin kit. The suspension was then transferred to a Lysing Matrix E tube also supplied in the FastDNA spin kit, and manufacturers' protocols subsequently followed precisely. DNA fragments in the size range 3 kb ~20 kb were isolated on a 1% "1x" Tris-borate-EDTA (TBE) gel stained with ethidium bromide to enable viewing under UV light (10x TBE solution from Invitrogen Ltd., UK). The DNA was extracted from the gel using a QIAquick gel extraction kit (QIAGEN Ltd., UK.).

A fragment of the 16s rRNA gene of approximately 500bp was amplified using using broad-specificity bacterial primers 8f (5´-AGAGTTTGATCCTGGCTCAG-3´) [13] and 519r (5´-GWATTACCGCGGCKGCTG-3´) where K = G or T, W = A or T [14]. Each PCR reaction mixture contained 20 µl of purified DNA solution, GoTaq DNA polymerase (5 units), 1× PCR reaction buffer, $MgCl_2$ (1.5mM), PCR nucleotide mix (0.2 mM), T4 Gene 32 Protein (100 ng/µl) and 8f and 519r primers (0.6 µM each) in a final volume of 50 µl. The reaction mixtures were incubated at 95°C for 2 min, and

then cycled 30 times through three steps: denaturing (95°C, 30 s), annealing (50°C, 30s), primer extension (72°C, 45 s). This was followed by a final extension step at 72°C for 7min. The PCR products were purified using a QIAquick PCR Purification Kit. Amplification product sizes were verified by electrophoresis of 10 µl samples in a 1.0% agarose TBE gel with ethidium bromide straining.

The PCR product was ligated into the standard cloning vector (pGEM-T Easy; Promega Corp., USA), and transformed into E. coli competent cells (XL1-Blue; Agilent Technologies UK Ltd). Transformed cells were grown on LB-agar plates containing ampicillin (100 $\mu g.ml^{-1}$) at 37°C for 17 hours. The plates were surfaced dressed with IPTG and X-gal (as per the XL1-Blue protocol) for blue-white colour screening. For each sample, 48 colonies containing a plasmid with the 16s rRNA gene insert were restreaked on LB-ampicillin agar plates and incubated at 37°C. 48 single colonies for each condition from restreaked plates were stab inoculated into an LB-agar ampicillin 96 well plate and sent for sequencing (GATC Biotech Ltd). In order to increase confidence that a suitable representation of the highly diverse B2 310 soil population had been collected, a further 16 plasmids were sent for sequencing. Single colonies from restreaked plates were incubated overnight at 37°C in LB media. Bacterial plasmids were then extracted from the resulting broth using the Promega Pureyield™ Plasmid Miniprep Purification system (Promega Corp., USA). The concentration of plasmid DNA was then determined using UV spectroscopy, and adjusted to 50 $ng.\mu l^{-1}$ with deionised water. 12µl of each plasmid mixture was then sent for sequencing at the Faculty of Biological Sciences, University of Leeds, Leeds, UK.

4.3 Phylogenic assignment.

16s rRNA bacterial sequence fragments, ~500 bp, of cloned DNA from B2 310 initial soil sample and isolated iron reducing consortium were checked with both Bellerophon[15] and Mallard v 1.02[16] online chimera checkers in order to exclude putative chimeras from subsequent analyses. Sequences were then assigned to bacterial phyla using the online Ribosomal Database Project (RDP) naïve Bayesian Classifier version 2.2 (available online: http://rdp.cme.msu.edu/classifier/classifier.jsp) in August 2010. The sequences were assigned to the taxonomical hierarchy: RDP training set 6, based on nomenclatural taxonomy and Bergey's Manual, with a confidence threshold

of 95% (assignments to a phylum reported in Figure 4 are based on >98% confidence). Full details of this algorithm, its development and its performance can be found in Wang et al., (2007)[17]

Supporting Information References

[1] B.A. Schumacher, Methods for the Determination of Total Organic Carbon (TOC) in Soils and Sediments, in, United States Environmental Protection Agency, Las Vegas, 2002.
[2] ASTM, D4972-01: standard test method for pH of soils. Annual book of ASTM standards, American Society for Testing and Materials, 4 (2006) 963-965.
[3] USEPA, SW-846 Manual: Method 7196a. Chromium hexavalent (colorimetric). Retrieved 6th Jan 2006, (1992).
[4] B. Ravel, M. Newville, ATHENA, ARTEMIS, HEPHAESTUS: data analysis for X-ray absorption spectroscopy using IFEFFIT, J. Synchrot. Radiat., 12 (2005) 537-541.
[5] A. Tenderholt, B. Hedman, K.O. Hodgson, PySpline: A modern, cross-platform program for the processing of raw averaged XAS edge and EXAFS data, in: B. Hedman, P. Painetta (Eds.) X-Ray Absorption Fine Structure-XAFS13, 2007, pp. 105-107.
[6] S. Tomic, B.G. Searle, A. Wander, N.M. Harrison, A.J. Dent, J.F.W. Mosselmans, J.E. Inglesfield, CCLRC Technical Report DL-TR-2005-001, ISSN 1362-0207(2005), in, 2005.
[7] S.J. Gurman, N. Binsted, I. Ross, A Rapid, Exact Curved-Wave Theory for Exafs Calculations, J. Phys. C. Solid State, 17 (1984) 143-151.
[8] N. Binsted, CLRC Daresbury Laboratory EXCURV98 program, CLRC Daresbury Laboratory, Warrington, UK, 1998.
[9] I.T. Burke, C. Boothman, J.R. Lloyd, R.J.G. Mortimer, F.R. Livens, K. Morris, Effects of progressive anoxia on the solubility of technetium in sediments, Environ. Sci. Technol., 39 (2005) 4109-4116.
[10] L. Charlet, A. Manceau, X-Ray Absorption Spectroscopic Study of the Sorption of Cr(Iii) at the Oxide Water Interface .2. Adsorption, Coprecipitation, and Surface Precipitation on Hydrous Ferric-Oxide, J. Colloid Interface Sci., 148 (1992) 443-458.
[11] N. Binsted, R.W. Strange, S.S. Hasnain, Constrained and Restrained Refinement in Exafs Data-Analysis with Curved Wave Theory, Biochemistry-US, 31 (1992) 12117-12125.
[12] R.A. Bruce, L.A. Achenbach, J.D. Coates, Reduction of (per)chlorate by a novel organism isolated from paper mill waste, Environ. Microbiol., 1 (1999) 319-329.
[13] P.A. Eden, T.M. Schmidt, R.P. Blakemore, N.R. Pace, Phylogenetic Analysis of Aquaspirillum-Magnetotacticum Using Polymerase Chain Reaction-Amplified 16s Ribosomal-Rna-Specific DNA, Int. J. Syst. Bacteriol., 41 (1991) 324-325.
[14] D.J. Lane, B. Pace, G.J. Olsen, D.A. Stahl, M.L. Sogin, N.R. Pace, Rapid determination of 16S ribosomal RNA sequences for phylogenetic analysis, P. Natl. Acad. Sci. USA, 82 (1985) 6955-6959.
[15] T. Huber, G. Faulkner, P. Hugenholtz, Bellerophon: a program to detect chimeric sequences in multiple sequence alignments, Bioinformatics, 20 (2004) 2317-2319.
[16] K.E. Ashelford, N.A. Chuzhanova, J.C. Fry, A.J. Jones, A.J. Weightman, New screening software shows that most recent large 16S rRNA gene clone libraries contain chimeras, Appl. Environ. Microbiol., 72 (2006) 5734-5741.
[17] Q. Wang, G.M. Garrity, J.M. Tiedje, J.R. Cole, Naive Bayesian classifier for rapid assignment of rRNA sequences into the new bacterial taxonomy, Appl. Environ. Microbiol., 73 (2007) 5261-5267.
[18] W.D. Derbyshire, H.J. Yearian, X-Ray Diffraction and Magnetic Measurements of the Fe-Cr Spinels, Phys. Rev., 112 (1958) 1603-1607.
[19] E. Doelsch, I. Basile-Doelsch, J. Rose, A. Masion, D. Borschneck, J.L. Hazemann, H. Saint Macary, J.Y. Borrero, New combination of EXAFS spectroscopy and density fractionation for the speciation of chromium within an andosol, Environ. Sci. Technol., 40 (2006) 7602-7608.

Table S1. Selected XRF major and trace elemental composition of soil samples reported as component oxide weight percent and parts per million (ppm) respectively. Major element data corrected for loss on ignition.

Borehole	Depth (cm)	Soil type	SiO_2	MgO	CaO	Fe_2O_3	Cr	As	Ba	Cu	Ni	Pb	Sn	Zn	Zr
B2	190-210	COPR Waste	2.25	6.31	46.63	5.54	12716	331.5	481	17.6	512.1	21.9	2.9	100.8	5.8
B2	310	Grey clay	58.79	1.21	6.12	5.70	3436	86.3	501.3	67.3	78.1	56	43.2	167.7	323.9
B2	320-340	Grey grey	56.81	1.39	4.23	6.13	3946	41.5	552.2	26.7	67.1	44.5	15.8	123.3	278.6
B2	365	Grey clay	78.61	0.36	0.69	4.39	846	17.1	348.9	23.5	28.8	21.2	9.9	76.6	393.2
B3	150-200	Topsoil	53.37	0.7	0.47	5.71	4890	432.6	631.5	655.1	35	596.9	1242.6	152.1	200.2
B3	200-240	Topsoil	54.92	0.73	0.96	6.08	4321	374.7	511.2	537.4	70.2	529	1412.4	710.5	201.9
B3	240-250	Brown clay	63.95	0.82	1.41	5.30	1431	109.5	528.3	38.7	44.9	69	68.6	155.4	322.7
B3	280-333	Brown clay	59.54	0.98	1.65	7.48	1511	28.9	448.5	31.7	46.8	28.3	2.1	140.2	290.9
B3	360-365	Grey clay	76.64	0.65	0.88	3.66	1379	26.2	371.7	22.4	25.2	25.2	12.8	64.5	401.7
B4	240-270	Grey clay	57.29	0.89	0.73	8.88	336	16.8	447.8	65.2	49.3	56.7	48.2	252.7	279.2
B4	270-280	Grey clay	81.57	0.39	0.19	3.61	847	6	361.6	176	40.6	27.2	10	652.6	308.9
B5	190-200	Brown clay	61.75	0.84	0.23	5.82	1599	6.7	467.6	138.5	103.6	42.2	1.3	984.2	298
B5	220-230	Grey clay	60.52	0.81	0.44	7.58	1278	6.6	491.6	226.6	128.3	47.4	1.5	2215	287.3
B6	220	Brown clay	81.1	0.4	0.16	3.97	162	6.2	341.2	36	38.7	21	4.5	491.6	339.4
BH402	8.8-9.0 m	Brown clay	53.43	0.98	3.02	8.71	8846	15.9	499.2	40.5	60	81	4.6	186.1	227.4
BH402	9.5-10.8 m	Grey clay	58.35	0.89	1.4	7.94	868	29.9	420	39.1	37.3	62.5	24	118.5	270.5

Table S2. RDP classification with 95% confidence threshold and OTU assignment for sequences obtained from B2 310 initial sample.

ID*	Accession number	Sequence length	Classification using the RDP classifier[17] (95% Confidence threshold)
BHL3-310I-1	FR695903	536	Firmicutes, Bacilli, Bacillales, Bacillaceae
BHL3-310I-2	FR695904	527	Proteobacteria, Betaproteobacteria
BHL3-310I-3	FR695905	547	Verrucomicrobia, Subdivision3, Subdivision3_genera_incertae_sedis
BHL3-310I-4	FR695906	470	Proteobacteria, Alphaproteobacteria
BHL3-310I-5	FR695907	517	Actinobacteria, Actinobacteria, Rubrobacteridae, Solirubrobacterales
BHL3-310I-6	FR695908	527	Proteobacteria, Betaproteobacteria
BHL3-310I-7	FR695909	535	Firmicutes, Bacilli, Bacillales, Bacillaceae, Bacillus
BHL3-310I-8	FR695910	527	Proteobacteria, Betaproteobacteria
BHL3-310I-9	FR695911	527	Proteobacteria, Betaproteobacteria
BHL3-310I-10	FR695912	499	Firmicutes, Clostridia, Clostridiales
BHL3-310I-11	FR695913	545	Verrucomicrobia, Subdivision3, Subdivision3_genera_incertae_sedis
BHL3-310I-12	FR695914	510	Firmicutes, Clostridia, Natranaerobiales, Natranaerobiaceae, Dethiobacter
BHL3-310I-14	FR695915	526	Nitrospira, Nitrospira, Nitrospirales, Nitrospiraceae, Nitrospira
BHL3-310I-15	FR695916	527	Bacteroidetes, Sphingobacteria, Sphingobacteriales, Chitinophagaceae
BHL3-310I-16	FR695917	510	Firmicutes, Clostridia, Natranaerobiales, Natranaerobiaceae, Dethiobacter
BHL3-310I-17	FR695918	531	Proteobacteria
BHL3-310I-18	FR695919	510	Firmicutes, Clostridia, Clostridiales, IncertaeSedisXIV, Anaerobranca
BHL3-310I-19	FR695920	517	Bacteroidetes, Flavobacteria, Flavobacteriales, Flavobacteriaceae, Flavobacterium
BHL3-310I-20	FR695921	525	Proteobacteria, Betaproteobacteria
BHL3-310I-21	FR695922	509	Actinobacteria, Actinobacteria, Actinobacteridae, Actinomycetales, Micrococcineae, Microbacteriaceae
BHL3-310I-22	FR695923	523	Bacteroidetes, Sphingobacteria, Sphingobacteriales, Chitinophagaceae
BHL3-310I-23	FR695924	549	Firmicutes, Clostridia, Clostridiales, Peptococcaceae, Peptococcaceae1, Desulfosporosinus
BHL3-310I-24	FR695925	525	Proteobacteria, Gammaproteobacteria
BHL3-310I-25	FR695926	522	-
BHL3-310I-26	FR695927	527	Proteobacteria, Betaproteobacteria, Burkholderiales
BHL3-310I-27	FR695928	532	Proteobacteria
BHL3-310I-28	FR695929	525	Proteobacteria, Betaproteobacteria
BHL3-310I-29	FR695930	517	Bacteroidetes, Flavobacteria, Flavobacteriales, Flavobacteriaceae, Flavobacterium
BHL3-310I-30	FR695931	500	Planctomycetes, Planctomycetacia, Planctomycetales, Planctomycetaceae, Gemmata
BHL3-310I-31	FR695932	536	Acidobacteria, Acidobacteria_Gp6, Gp6
BHL3-310I-32	FR695933	515	Bacteroidetes, Flavobacteria, Flavobacteriales, Flavobacteriaceae, Flavobacterium
BHL3-310I-34	FR695934	542	Nitrospira, Nitrospira, Nitrospirales, Nitrospiraceae, Leptospirillum
BHL3-310I-35	FR695935	509	Actinobacteria, Actinobacteria
BHL3-310I-36	FR695936	525	Proteobacteria, Betaproteobacteria
BHL3-310I-37	FR695937	507	Actinobacteria, Actinobacteria, Actinobacteridae, Actinomycetales, Micrococcineae
BHL3-310I-38	FR695938	528	Bacteroidetes, Sphingobacteria, Sphingobacteriales, Chitinophagaceae, Ferruginibacter
BHL3-310I-39	FR695939	543	
BHL3-310I-40	FR695940	536	Proteobacteria, Deltaproteobacteria, Myxococcales, Nannocystineae
BHL3-310I-41	FR695941	526	Nitrospira, Nitrospira, Nitrospirales, Nitrospiraceae, Nitrospira
BHL3-310I-42	FR695942	526	Proteobacteria, Betaproteobacteria
BHL3-310I-43	FR695943	508	Planctomycetes, Planctomycetacia, Planctomycetales, Planctomycetaceae
BHL3-310I-44	FR695944	531	Actinobacteria, Actinobacteria, Rubrobacteridae, Solirubrobacterales
BHL3-310I-45	FR695945	549	Firmicutes, Clostridia, Clostridiales, Peptococcaceae, Peptococcaceae1, Desulfosporosinus
BHL3-310I-46	FR695946	541	
BHL3-310I-47	FR695947	541	
BHL3-310I-48	FR695948	510	

ID*	Accession number	Sequence length	Classification using the RDP classifier[17] (95% Confidence threshold)
BHL3-310I-49	FR695949	510	Firmicutes, Clostridia, Natranaerobiales, Natranaerobiaceae, Dethiobacter
BHL3-310I-50	FR695950	527	Proteobacteria, Betaproteobacteria
BHL3-310I-51	FR695951	522	Bacteroidetes, Sphingobacteria, Sphingobacteriales, Cyclobacteriaceae
BHL3-310I-52	FR695952	531	
BHL3-310I-53	FR695953	522	Bacteroidetes, Sphingobacteria, Sphingobacteriales, Cyclobacteriaceae
BHL3-310I-54	FR695954	531	Proteobacteria
BHL3-310I-55	FR695955	527	Proteobacteria, Betaproteobacteria
BHL3-310I-56	FR695956	512	Firmicutes, Clostridia, Clostridiales, IncertaeSedisXIV, Anaerobranca
BHL3-310I-57	FR695957	523	Bacteroidetes
BHL3-310I-58	FR695958	532	Actinobacteria, Actinobacteria, Rubrobacteridae, Solirubrobacterales, Solirubrobacteraceae, Solirubrobacter
BHL3-310I-59	FR695959	513	Bacteria_incertae_sedis, Ktedonobacteria, Ktedonobacterales, Ktedonobacteraceae, Ktedonobacter
BHL3-310I-60	FR695960	510	Firmicutes, Clostridia, Natranaerobiales, Natranaerobiaceae, Dethiobacter
BHL3-310I-61	FR695961	516	Proteobacteria, Betaproteobacteria, Burkholderiales, Comamonadaceae, Pelomonas
BHL3-310I-62	FR695962	521	Firmicutes, Clostridia, Clostridiales, IncertaeSedisXI, Tissierella
BHL3-310I-63	FR695963	537	Firmicutes, Bacilli, Bacillales, Bacillaceae, Bacillus
BHL3-310I-64	FR695964	474	Proteobacteria, Alphaproteobacteria, Rhizobiales

* BHL3 was renumbered B2 after sequences had been submitted to GenBank

Table S3. RDP classification with 95% confidence threshold and OTU assignment for sequences obtained from iron reducing consortium isolated from B2 310 sample.

ID*	Accession number	Sequence length	Classification using the RDP classifier[17] (95% Confidence threshold)
BHL3_Fe_Consort_1	FR820910	521	Firmicutes, Clostridia, Clostridiales, Incertae Sedis XI, Tissierella
BHL3_Fe_Consort_2	FR820911	511	
BHL3_Fe_Consort_3	FR820912	516	Firmicutes, Clostridia, Clostridiales, Clostridiaceae
BHL3_Fe_Consort_4	FR820913	506	Firmicutes, Clostridia, Clostridiales, Clostridiaceae, Clostridiaceae 2, Natronincola
BHL3_Fe_Consort_5	FR820914	516	Firmicutes, Clostridia, Clostridiales, Clostridiaceae
BHL3_Fe_Consort_6	FR820915	512	Firmicutes, Clostridia, Clostridiales, Incertae Sedis XIV, Anaerobranca
BHL3_Fe_Consort_7	FR820916	517	Firmicutes, Clostridia, Clostridiales, Clostridiaceae
BHL3_Fe_Consort_8	FR820917	516	Firmicutes, Clostridia, Clostridiales, Clostridiaceae
BHL3_Fe_Consort_9	FR820918	514	Firmicutes, Clostridia
BHL3_Fe_Consort_10	FR820919	515	Firmicutes, Clostridia, Clostridiales, Clostridiaceae
BHL3_Fe_Consort_11	FR820920	521	Firmicutes, Clostridia, Clostridiales, Incertae Sedis XI, Tissierella
BHL3_Fe_Consort_12	FR820921	516	Firmicutes, Clostridia, Clostridiales, Clostridiaceae
BHL3_Fe_Consort_13	FR820922	496	Firmicutes
BHL3_Fe_Consort_14	FR820923	516	Firmicutes, Clostridia, Clostridiales, Clostridiaceae
BHL3_Fe_Consort_15	FR820924	516	Firmicutes, Clostridia, Clostridiales, Clostridiaceae
BHL3_Fe_Consort_16	FR820925	586	Firmicutes, Clostridia, Clostridiales
BHL3_Fe_Consort_17	FR820926	516	Firmicutes, Clostridia, Clostridiales, Clostridiaceae
BHL3_Fe_Consort_18	FR820927	557	Firmicutes, Clostridia, Clostridiales, Peptococcaceae, Peptococcaceae 1, Desulfitibacter
BHL3_Fe_Consort_19	FR820928	521	Firmicutes, Clostridia, Clostridiales
BHL3_Fe_Consort_20	FR820929	521	Firmicutes, Clostridia, Clostridiales, Incertae Sedis XI
BHL3_Fe_Consort_21	FR820930	518	Firmicutes, Clostridia, Clostridiales, Incertae Sedis XIV, Anaerovirgula
BHL3_Fe_Consort_22	FR820931	589	Firmicutes, Clostridia, Clostridiales
BHL3_Fe_Consort_23	FR820932	512	Firmicutes, Clostridia, Clostridiales, Incertae Sedis XIV, Anaerobranca
BHL3_Fe_Consort_24	FR820933	521	Firmicutes, Clostridia, Clostridiales
BHL3_Fe_Consort_25	FR820934	518	Firmicutes, Clostridia, Clostridiales, Incertae Sedis XIV, Anaerovirgula
BHL3_Fe_Consort_26	FR820935	511	
BHL3_Fe_Consort_27	FR820936	584	Firmicutes, Clostridia, Clostridiales
BHL3_Fe_Consort_28	FR820937	512	Firmicutes, Clostridia, Clostridiales, Incertae Sedis XIV, Anaerobranca
BHL3_Fe_Consort_30	FR820938	521	Proteobacteria, Betaproteobacteria, Burkholderiales, Comamonadaceae, Comamonas
BHL3_Fe_Consort_31	FR820939	512	Firmicutes, Clostridia, Clostridiales, Incertae Sedis XIV, Anaerobranca
BHL3_Fe_Consort_32	FR820940	583	Firmicutes, Clostridia, Clostridiales
BHL3_Fe_Consort_33	FR820941	630	Firmicutes, Clostridia, Clostridiales, Incertae Sedis XIV, Anaerovirgula
BHL3_Fe_Consort_34	FR820942	582	Firmicutes, Clostridia, Clostridiales, Incertae Sedis XIV, Anaerobranca
BHL3_Fe_Consort_35	FR820943	511	Firmicutes, Clostridia, Clostridiales, Incertae Sedis XIV, Anaerobranca
BHL3_Fe_Consort_36	FR820944	516	Firmicutes, Clostridia, Clostridiales, Clostridiaceae
BHL3_Fe_Consort_37	FR820945	516	Firmicutes, Clostridia, Clostridiales, Clostridiaceae
BHL3_Fe_Consort_38	FR820946	512	Firmicutes, Clostridia, Clostridiales, Incertae Sedis XIV, Anaerobranca
BHL3_Fe_Consort_39	FR820947	521	Firmicutes, Clostridia, Clostridiales, Peptococcaceae
BHL3_Fe_Consort_40	FR820948	512	Firmicutes, Clostridia, Clostridiales, Incertae Sedis XIV, Anaerobranca
BHL3_Fe_Consort_41	FR820949	584	Firmicutes, Clostridia, Clostridiales
BHL3_Fe_Consort_42	FR820950	521	Firmicutes, Clostridia, Clostridiales, Incertae Sedis XI, Tissierella
BHL3_Fe_Consort_43	FR820951	516	Firmicutes, Clostridia, Clostridiales, Clostridiaceae, Clostridiaceae 2, Alkaliphilus
BHL3_Fe_Consort_44	FR820952	516	Firmicutes, Clostridia, Clostridiales, Clostridiaceae
BHL3_Fe_Consort_45	FR820953	516	Firmicutes, Clostridia, Clostridiales, Clostridiaceae
BHL3_Fe_Consort_46	FR820954	511	Firmicutes
BHL3_Fe_Consort_47	FR820955	504	
BHL3_Fe_Consort_48	FR820956	516	Firmicutes, Clostridia, Clostridiales, Clostridiaceae

* BHL3 was renumbered B2 after sequences had been submitted to GenBank

Table S4. Idealised Cr molecular co-ordination environment in the chromite structure where n is the number of atoms in each shell and R is the bond distance. Calculated from structural information presented in Derbyshire et al. [18].

Structure	Shell	n	R (Å)
Chromite	O	6	1.99
	Cr-Cr	6	2.97
	Cr-Fe	6	3.47

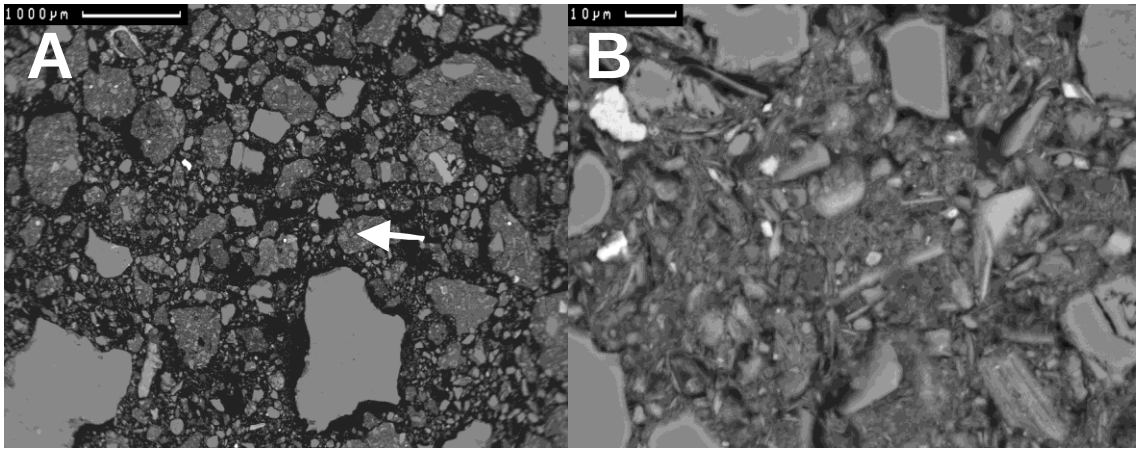

Figure S1. Backscatter SEM images of resin embedded thin section from B2-310 soil sample, showing (A) low magnification view of angular quartz grains in a fine grained matrix (scale bar 1000 µM); (B) higher magnification view (from white arrow, frame A) of fine grained clay-like matrix material (scale bar 10 µM).

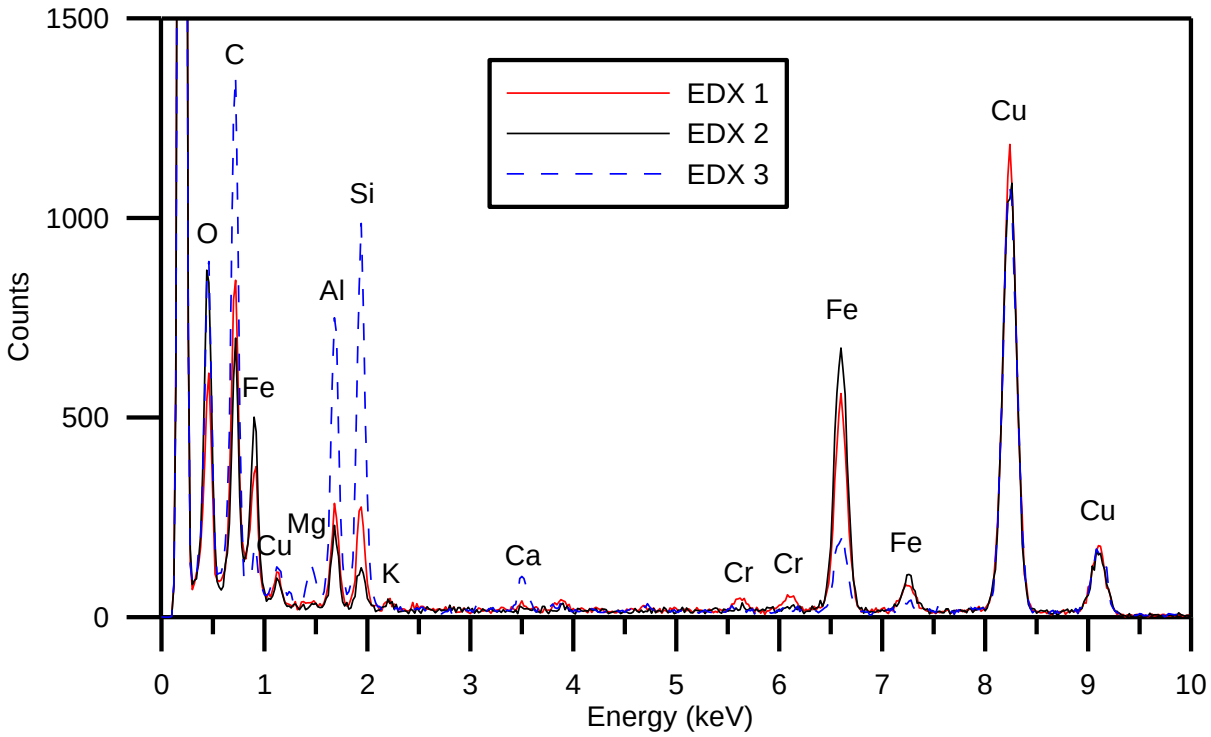

Figure S2. Point EDX spectra (10-20 nm probe diameter) from the 3 localities identified by STEM imaging (see Figure 4, main text): Point 1, Fe-rich, Cr containing oxide hotspot (red); Point 2 Fe-rich oxide particle (black); Particle 3 Si and Al rich oxide particle (blue).

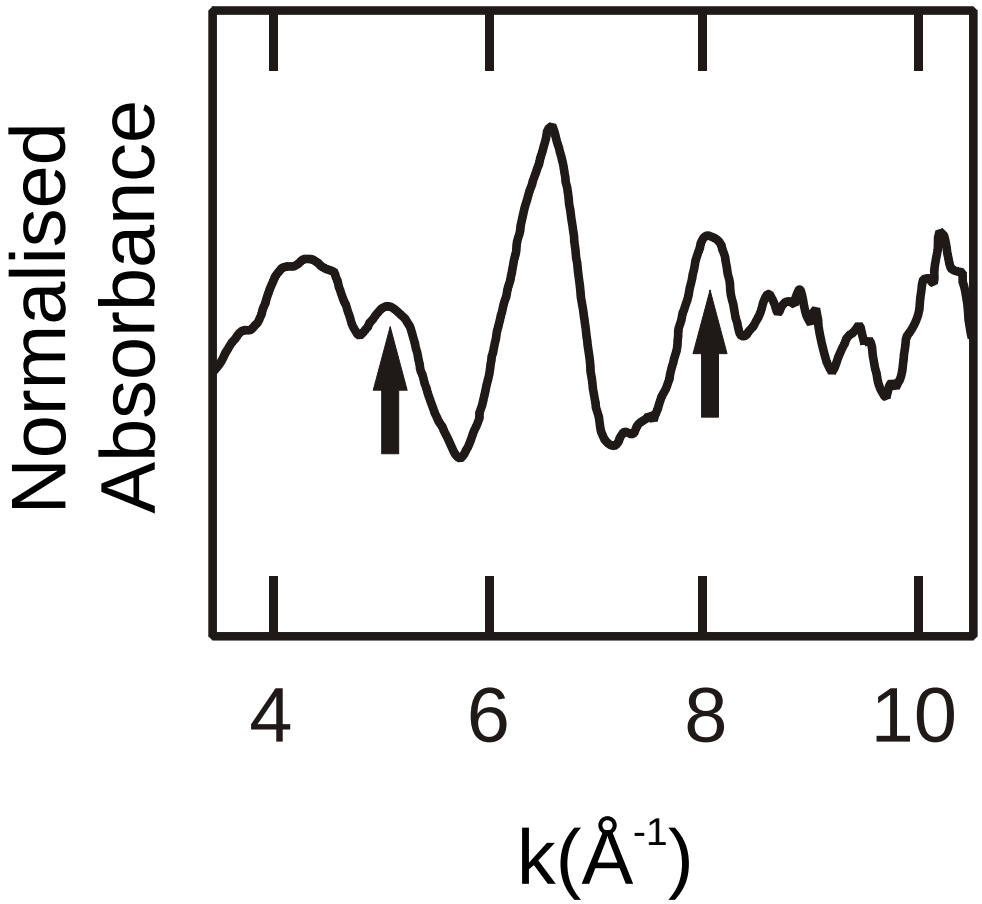

Figure S3. Chromite ore Cr K-edge EXAFS spectra. Arrows highlight the characteristic sub peak features at k=5.1 and 8 $Å^{-1}$, redrawn from Doelsch et al. [19].